

Supporting Information

MXene Nanosheet-Based Microneedles for Monitoring Muscle Contraction and Electrostimulation Treatment

Yen-Chang Yang ^{a #}, Yen-Tzu Lin ^{a #}, Jiasheng Yu ^b, Huan-Tsung Chang ^c, Ting-Yu Lu ^b, Tzu-Yen Huang ^d, Anant Preet ^{c,e}, Ya-Ju Hsu ^c, Ligang Wang ^{f, g}, and Tzu-En Lin ^{a *}

a Institute of Biomedical Engineering, College of Electrical and Computer Engineering, National Yang Ming Chiao Tung University, 30010 Hsinchu, Taiwan

b Department of Chemical Engineering, National Taiwan University, Taipei 10617, Taiwan
No.1, Section 4, Roosevelt Road, Taipei, Taiwan

c Department of Chemistry, National Taiwan University, Taipei 10617, Taiwan
No.1, Section 4, Roosevelt Road, Taipei, Taiwan

d International Thyroid Surgery Center, Department of Otolaryngology-Head and Neck Surgery, Kaohsiung Medical University Hospital, Kaohsiung Medical University, Kaohsiung 80756, Taiwan

e Chemical Biology and Molecular Biophysics Program, Taiwan International Graduate Program, Institute of Biological Chemistry, Academia Sinica, Nankang, Taipei, 115, Taiwan

f Group of Energy Materials, École Polytechnique Fédérale de Lausanne (EPFL), Valais Wallis, CH-1950 Sion, Switzerland

g Innovation Research Institute of Energy and Power, North China Electric Power University, Beinong Rd 2, Beijing, China

These authors contributed equally to this work.

* CORRESPONDING AUTHOR FOOTNOTE

EMAIL: telin@nctu.edu.tw

Telephone number: +886 (03)5731750

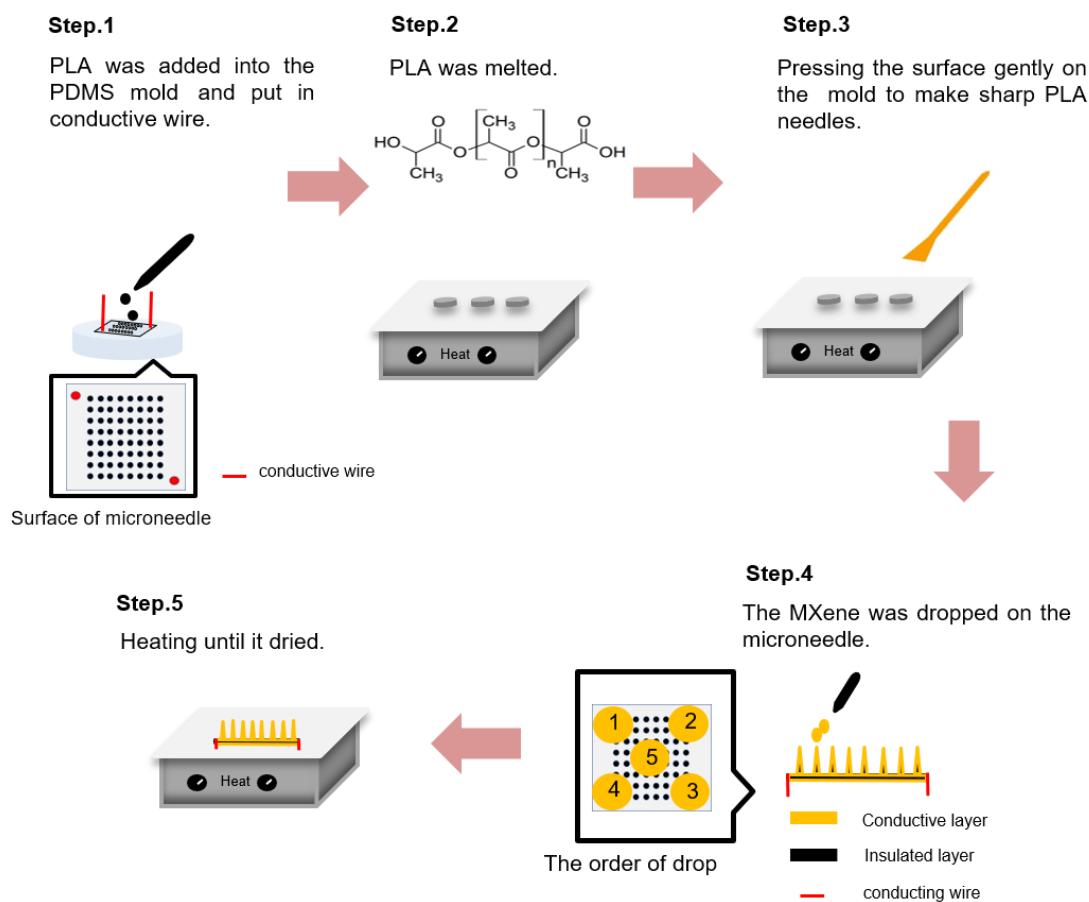
Address: No. 1001, Room 556B, Engineering Building 6, University Road,
Institute of Biomedical Engineering, National Yang Ming Chiao Tung University,
30010 Hsinchu, Taiwan.

Supporting Information

Table of content

S1 The fabrication processes of the microneedle.....	S-3
S2 The theory of eye movement measurement.....	S-4
S3 The microneedle fabricated by PLA plastic bags.....	S-6
S4 The cell toxicity test of MXene microneedle.....	S-6
S5 The stability of MXene microneedle, PEDOT:PSS microneedle, and traditional conductive hydrogel.....	S-8
S6 The video of the biosensing the muscle contraction on the human arm.....	S-10
S7 The fabrication of the electrostimulator.....	S-11
S8 The video of the contraction of the muscle induced by electrostimulation on the swine.....	S-12
S9 The coagulation experiments on the swine skin.....	S-13
References.....	S-13

S1 The fabrication processes of the microneedle



Scheme S1 The schematic representation for the fabrication of the MXene-coated microneedle. Firstly, the PLA was added to the mold and melted on the heater. In the second step, MXene solution was dropped on the microneedle and continued heating until it was dry.

The microneedle was fabricated using the polymer casting into the PDMS mold purchased from MICROPOINT (Singapore). For the fabrication of the polylactic acid (PLA) base, the solid powder of PLA was placed on the PDMS mold and heated to 185 °C for 0.5 hour on a hot plate (PLA melting point = 180 °C). After the PLA melted, a certain pressure was applied on the PLA through a flat iron plate for removing the air between the PLA and the PDMS mold. Then, more PLA powder was placed on the mold for filling up the microneedle-shaped grooves. The electric wires were inserted into the PLA vertically and continuously heated for another hour. Finally, 25 µm of the MXene stock solution was drop coated on the center and each corner of the microneedle, respectively. It was heated until it dried well (as shown in **Scheme S1**). If all the MXene solutions were dropped on the center of the microneedle, it would generate cracks and be non-uniformly coated. Therefore, fabricating a MXene nanosheet-based microneedle with high quality requires much technical knowledge.

If the MXene stock solution was not drop coated as we described

previously, the cracks would appear after it dried. We also tried other coating methods, such as spin coating, but the microneedle surface was still inhomogeneous and full of cracks. **Figure S1a** illustrated the cracks on the MXene nanosheet-based microneedle from a failed experiment. **Figure S1b** displays another defective microneedle without the sharp needle tip because the PLA was not pressed during the casting procedure.

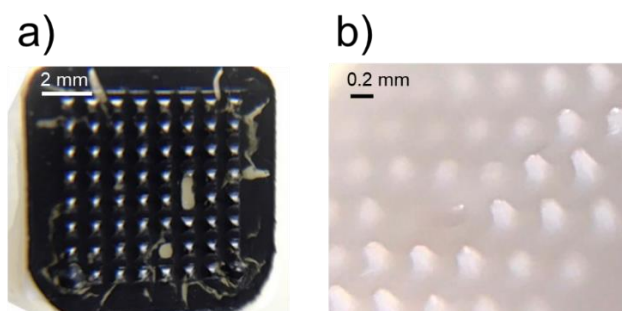


Figure S1 a) Defective MXene nanosheet-based microneedles with cracks and inhomogeneous coating. b) Defective microneedle without sharp needle tip.

The microneedles designed in this research are disposable, and MXene and PLA used in this research are all degradable materials, so they are environmentally friendly. Although the microneedle will cause no damage to the dermal layer so there will not blood in general; after the microneedle puncture, the microneedles should be collected and sealed in a hard container as medical waste.

S2 The theory of eye movement measurement

The principle of eye movement measurement (EOG) is described in **Figure S2** and **Scheme S2**. The potential difference between the cornea and the retina could generate an electric dipole. The cornea is positively charged, and the retina is negatively charged. If the eyeball rotates, weak potential differences (about 50~3500 μV) could be detected. Some disabled or visually impaired patients can still control their eye movement.¹ This technique has great potential for developing human-machine interface systems for communication.^{2,3} It is also pointed out in the literature that this system can also be used to monitor patients with sleep disorders. Also, patients with Parkinson's disease can use EOG to help monitor them. We used AD620 as an instrumentation amplifier with good anti-noise and DC offset, plus a low pass filter to filter out unnecessary signals, and the EOG signal can be displayed on the monitor (**Figure S3**).⁴

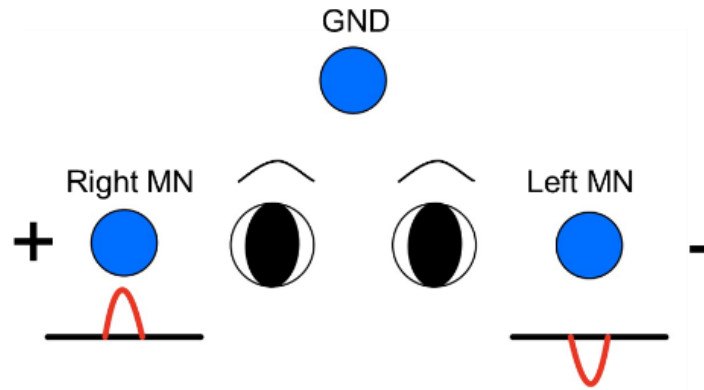
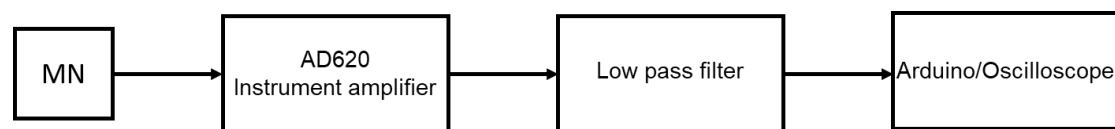


Figure S2 The figure shows the schematic diagram of the electrode placement. Place the positive and negative MN next to the right eye and the left eye. GND can be placed on the forehead or far away from the body. When the eyeball moves to the right, a positive wave peak appears. Otherwise, it moves to the left, negative crest.



Scheme S2 The flow chart illustrates the entire EOG signal acquisition process. The signal is collected by the microneedle electrode (MN) and amplified by the instrumentation amplifier, and then filtered through the filter to show the waveform on the monitor.

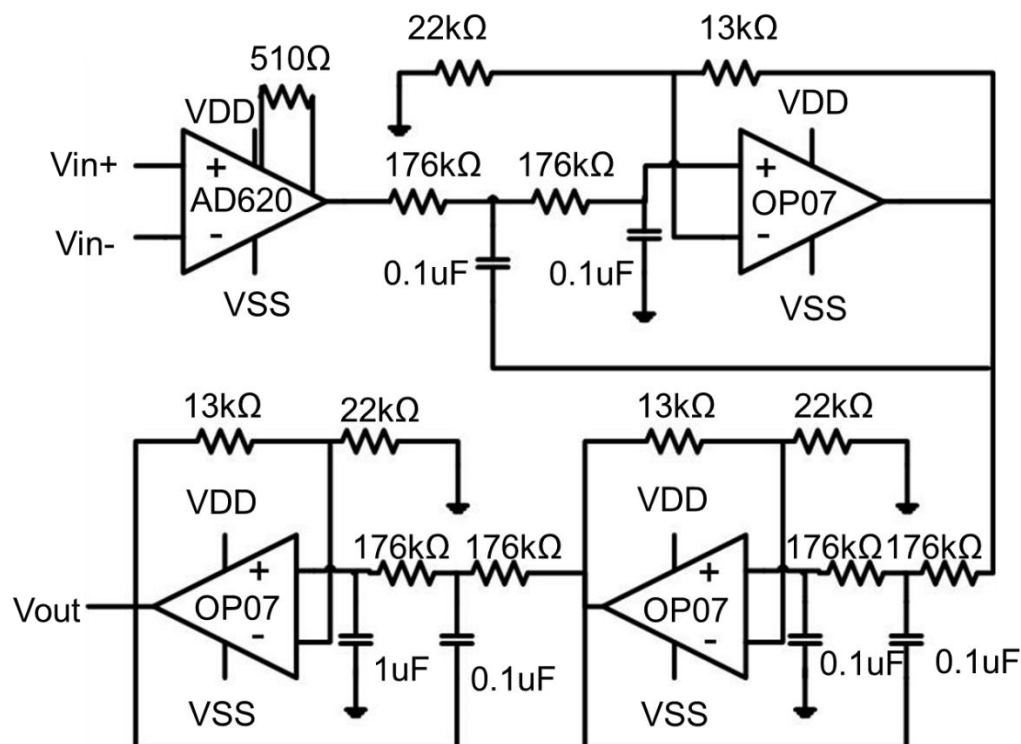


Figure S3 EOG measurement circuit diagram.

For the measurement process, please see the supplementary video SI 2.

This video shows the volunteer using microneedle electrodes around his eyes. The electrodes recorded the voltage signals generated from the movement of his eyeballs from left to the right. Furthermore, the volunteer's head shaking does not affect detecting EOG signal.

S3 The microneedle fabricated by PLA plastic bags

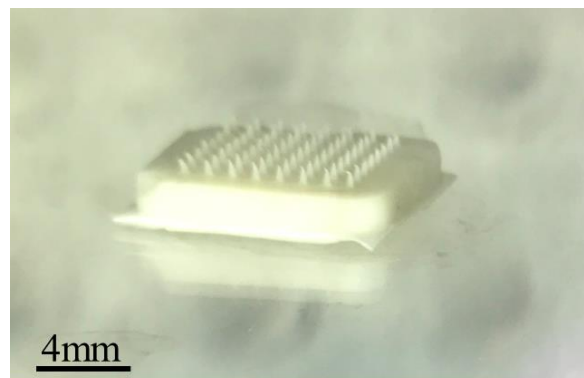


Figure S4 The microneedle fabricated by PLA plastic bags.

S4 The biocompatibility test of MXene microneedle

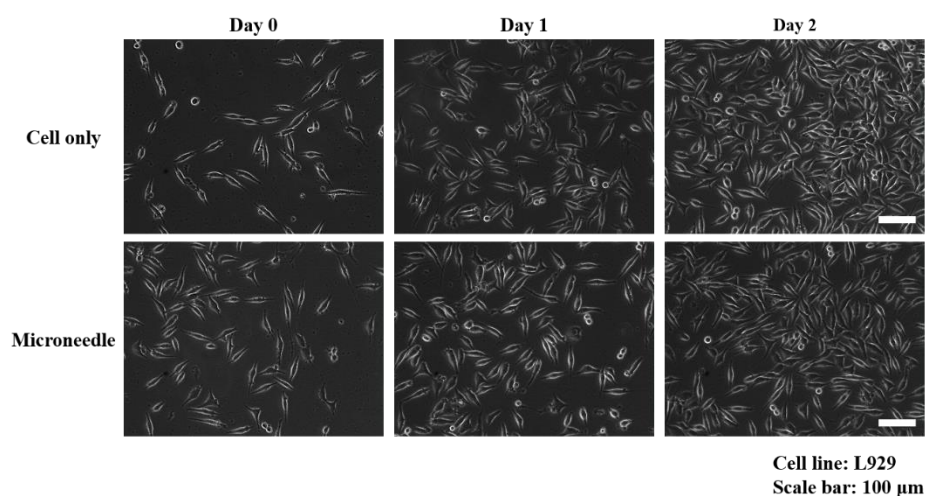


Figure S5 The cell morphology of L929 cells after co-incubating with microneedles.

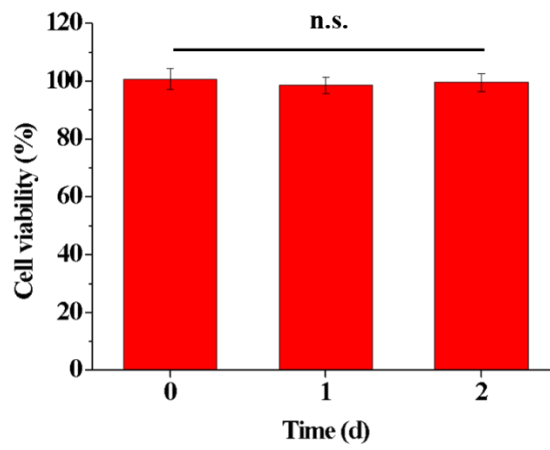


Figure S6 Cell viability of microneedle against L929 cells. (n.s. = no significant difference).

S5 The stability of MXene microneedle, PEDOT:PSS microneedle, and traditional conductive hydrogel

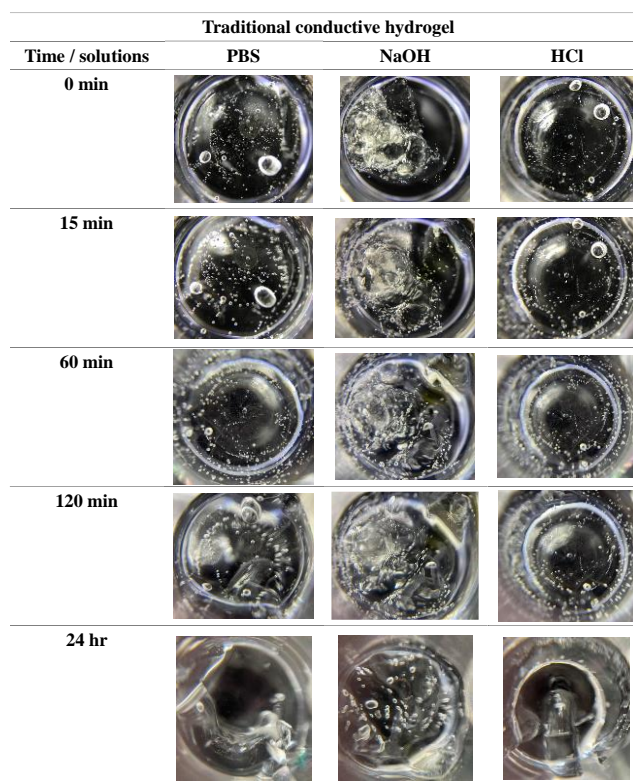


Figure S7 The traditional conductive hydrogel used in clinics could not resist salts (PBS), NaOH (pH 12) or, HCl (pH 2). It dissolved into the solution and denatured after immersing in the solution for few minutes.

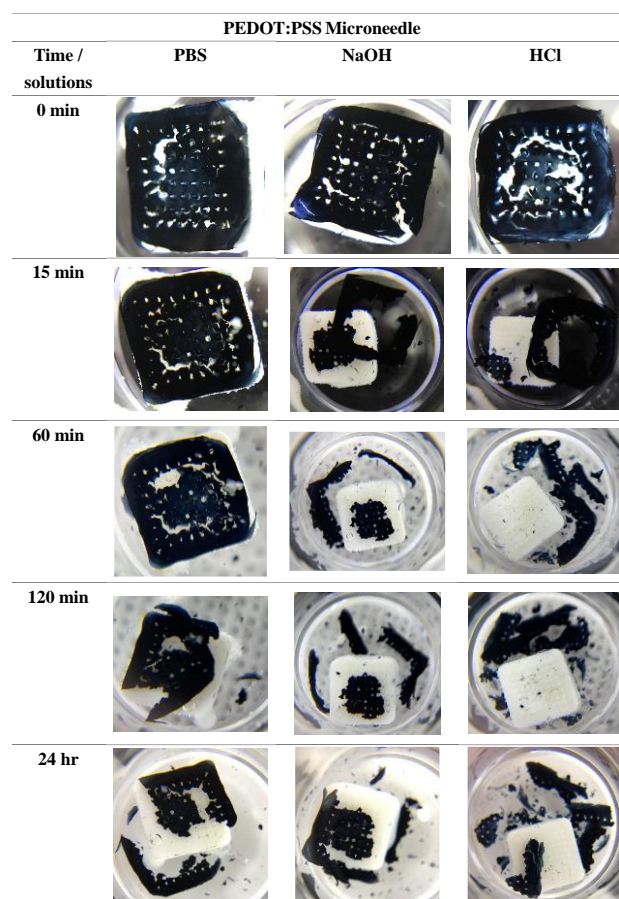


Figure S8 The PEDOT:PSS microneedles were immersed in PBS, HCl (pH 2), and NaOH (pH12) solutions. PEDOT:PSS decomposed after few hours of immersing in the solutions.

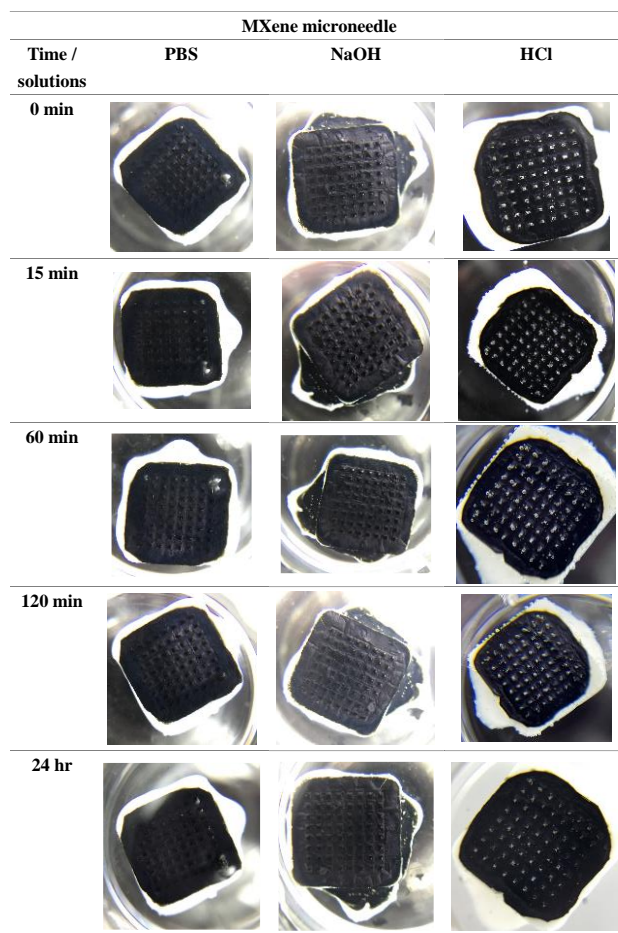


Figure S9 The MXene microneedles were immersed in PBS, HCl (pH 2), and NaOH (pH 12) solutions. Surprisingly, MXene microneedle was intact after immersing in these solutions.

S6 The video of the biosensing the muscle contraction on the human arm

The *supplimentary video (SI 6)* describes that MXene microneedles can be attached to bandages and then, placed onto a person's head and/or arms for sensing the eye movements as well as muscle contractions that result in voltage changes.

S7 The fabrication of the electrostimulator

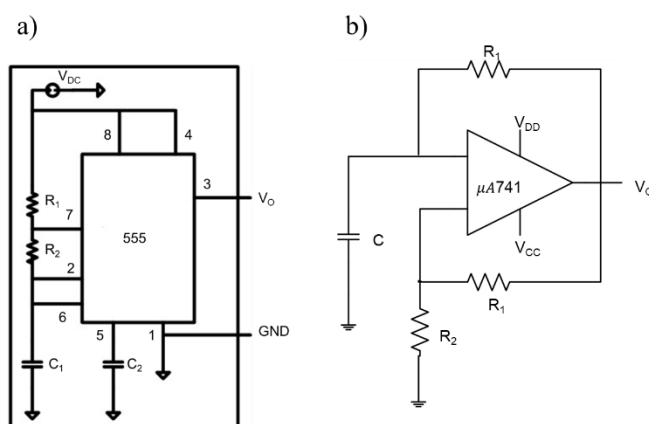


Figure S10 a) We can change the power (V_{DC}) to 5~9 V to control the output voltage, and we can rely on C_1 charge and discharge to control the square waveform transition, change R_1 , R_2 , C_1 can help design the waveform. b) We use the other IC, which is $\mu A741$ to set V_{DD} to 9 V, V_{CC} to -9 V to obtain a high voltage to flow the thick skin of swine and adjust the ratio of R_1 , R_2 to decide the period.

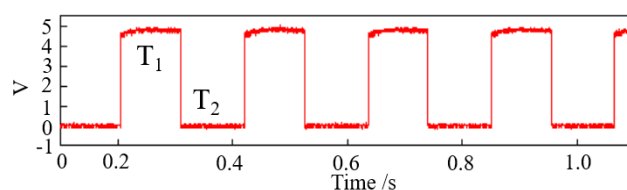


Figure S11 The output waveform of the voltages for the electrostimulation.

The circuit for electrostimulation adopted the combination of 555 oscillators, resistors (R), and capacitors (C). The formulas (1), (2), and (3) indicate that the period (T) of square waves of the voltages can be adjusted by setting the R_1 、 R_2 、 C_1 values when the C_2 was fixed to $0.01\mu F$. Thus, the amplitude of the square wave generated from this circuit is 4.7 V. Each duration is 213 ms, under the applied power source of 5V (V_{DC}).

$$T_1=0.693(R_1+R_2)\times C_1\ldots\ldots\ldots(1)$$

$$T_2=0.693\times R_2\times C_1\ldots\ldots\ldots(2)$$

$$T=T_1+T_2=0.693(R_1+2R_2)\times C_1\ldots\ldots\ldots(3)$$

Where GND means ground and V_O means output voltage.

S8 The video of the contraction of the muscle induced by electrostimulation on the swine

The supplementary video SI 8 demonstrates how MXene microneedles can be positioned on the nerve nearby the trachea of the swine for generating electrical pulses transmitted to that nerve using an electrostimulator.

Regarding to the experimental methods, they were described below. To induce the general anesthesia in the swine, 2-4% of sevoflurane at a fresh gas flow of 3 L/min was applied via the face mask with the piglet in a prone position. An adequate depth of anesthesia was achieved in 3-5 minutes. No severe movement confirmed the depth of anesthesia to pain due to peripheral venous catheterization. A superficial vein on the outer side of one ear was identified. The selected region (about 6 x 6 cm²) was sterilized with 75% alcohol. For achieving maximum safety, a 24-gauge peripheral intravenous catheter was used. Intravenous anesthetic, such as propofol (1-2 mg/kg), or thiamylal (5-10 mg/kg), was administered by the direct laryngoscopy to alleviate noxious stimulation. To maintain the anesthesia of the swine, the electrodes were fixed and positioned the piglet on its back with the neck extended, and the general anesthesia was carried out with sevoflurane 1-3% in oxygen 2 L/min. The lungs were ventilated in volume-control mode at a tidal volume of 8-12 mL/kg, and the respiratory rate was set to 12-14 breaths/min. The physiological reactions, including capnography, electrocardiography (ECG), and oxygenation (SaO₂), were monitored. The neck surgery was performed on the swine. The microneedles were placed on the muscles near the trachea. Afterward, we placed the microneedles on the muscles and observed the contraction. The electrical stimulation was set 4 times per second to induce the contraction of the intrinsic laryngeal muscles.

S9 The coagulation experiments on the swine skin

We created an injury with 0.5 cm depth using a #11 surgical scalpel blade on the skin of the swine. The natural coagulation time was more than 2 minutes. However, if we stimulated the electrical vasoconstriction, the coagulation time may be shortened to 50 seconds.

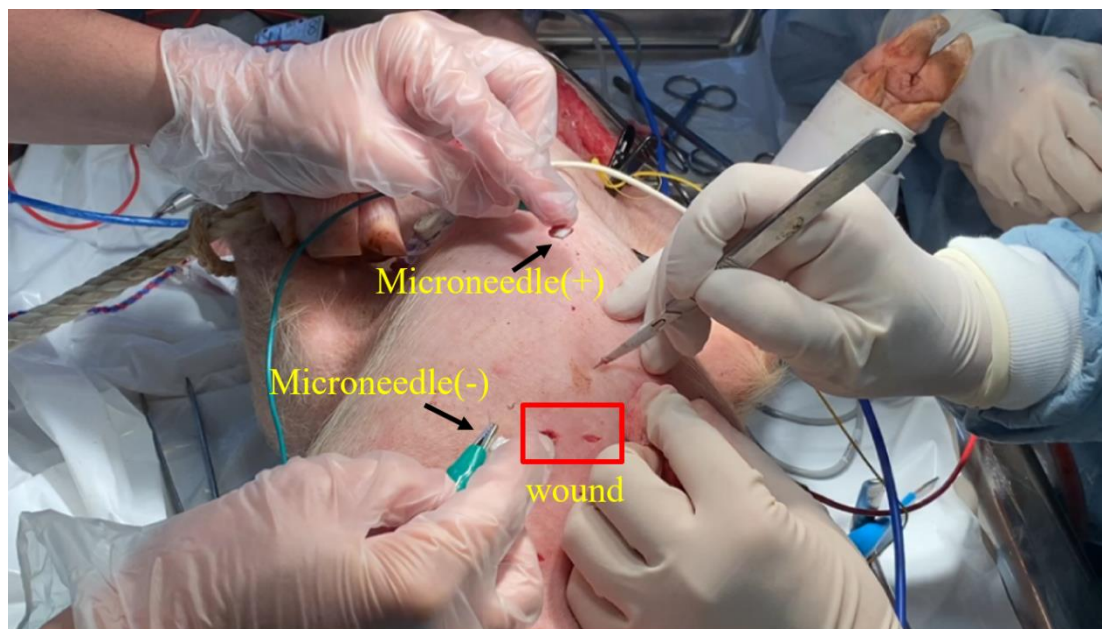


Figure S12 The microneedle system, coupled with electrical stimulation, could accelerate blood coagulation.

References:

- (1) Barea, R.; Boquete, L.; Ortega, S.; López, E.; Rodríguez-Ascariz, J. M. EOG-Based Eye Movements Codification for Human Computer Interaction. *Expert Systems with Applications* **2012**, 39 (3), 2677–2683. <https://doi.org/10.1016/j.eswa.2011.08.123>.
- (2) Stuart, S.; Hickey, A.; Galna, B.; Lord, S.; Rochester, L.; Godfrey, A. ITrack: Instrumented Mobile Electrooculography (EOG) Eye-Tracking in Older Adults and Parkinson's Disease. *Physiological Measurement* **2017**, 38 (1), N16. <https://doi.org/10.1088/1361-6579/38/1/N16>.
- (3) Christensen, J. A. E.; Zoetmulder, M.; Koch, H.; Frandsen, R.; Arvastson, L.; Christensen, S. R.; Jennum, P.; Sorensen, H. B. D. Data-Driven Modeling of Sleep EEG and EOG Reveals Characteristics Indicative of Pre-Parkinson's and Parkinson's Disease. *Journal of Neuroscience Methods* **2014**, 235, 262–276. <https://doi.org/10.1016/j.jneumeth.2014.07.014>.
- (4) Prabha, L.; Kayalvizhi, R.; Lashya, K.; Rajeswari, B. Eog Based Hand Controlled Glove Designed Using Arduino. *Journal of International Pharmaceutical Research* **2019**, 46 (4), 80–85.